

## Doping effect in layer structured $\text{SrBi}_2\text{Nb}_2\text{O}_9$ ferroelectrics

Yun Wu, Mike J. Forbess, Seana Seraji, Steven J. Limmer, Tammy P. Chou, Carolyn Nguyen, and Guozhong Cao<sup>a)</sup>

*Department of Materials Science and Engineering, University of Washington, Seattle, Washington 98195*

(Received 31 May 2001; accepted for publication 27 August 2001)

This article reports a systematic study of doping effects on the crystal structure, microstructure, dielectric, and electrical properties of layer-structured strontium bismuth niobate,  $\text{SrBi}_2\text{Nb}_2\text{O}_9$  (SBN), ferroelectrics. Substitution in both the A site ( $\text{Sr}^{2+}$  by  $\text{Ca}^{2+}$  and  $\text{Ba}^{2+}$ ) and B site ( $\text{Nb}^{5+}$  by  $\text{V}^{5+}$ ) up to 30 at % were studied. It was found that crystal lattice constant, dielectric, and electrical properties of SBN ferroelectrics varied appreciably with the type and amount of dopants. The relationships among the ionic radii, structural constraint imposed by  $[\text{Bi}_2\text{O}_2]^{2+}$  interlayers, and properties were discussed. © 2001 American Institute of Physics. [DOI: 10.1063/1.1413236]

### I. INTRODUCTION

Since the first studies by Aurivillius, the family of bismuth layer structured ferroelectrics (BLSFs) has been investigated extensively, because of its promise for ferroelectric random access memories applications.<sup>1–4</sup> The general formula for BLSFs is  $\text{Bi}_2\text{A}_{m-1}\text{B}_m\text{O}_{m+3}$ , where A=Bi, Pb, Na, K, Sr, Ca, Ba, rare earths; B=Ti, Nb, Ta, Fe, Mo, W, Cr; and  $m=1, 2, 3, 4, 5, 6$ .<sup>5</sup> This reflects the fact that there exists a good possibility for mutual dopings within these various elements or with some other ions to BLSFs. Generally, the doping could be in bismuth oxide layer and/or in perovskite-like units (A or B sites). A lot of work has been reported on the doping effect on the improvement of physical properties in BLSFs. Millan *et al.* reported the substitution of  $\text{Br}^{3+}$  in  $[\text{Bi}_2\text{O}_2]^{2+}$  layers by other cations such as  $\text{Pb}^{2+}$ ,  $\text{Sb}^{3+}$ ,  $\text{Sn}^{2+}$ , or  $\text{Te}^{4+}$ .<sup>6–8</sup> Within the perovskite-like units, partial substitution of strontium ions by bismuth ions would increase the Curie temperature and improve the dielectric properties in both strontium bismuth tantalate,  $\text{SrBi}_2\text{Ta}_2\text{O}_9$  (SBT) and SBN.<sup>9–11</sup> Subbarao reported that the Curie transition temperature decreases when the size of A site cations in BLSFs increases.<sup>12–14</sup> Newnham *et al.* reported the structure of 10 at % of  $\text{Sr}^{2+}$  substituted by  $\text{Ba}^{2+}$  in SBT with lower Curie temperature and reduced distortions in the perovskite units.<sup>15</sup> Properties of barium incorporated SBT thin films were also reported.<sup>16,17</sup> It was also found that SBN doping with  $\text{Ca}^{2+}$  resulted in an appreciable increase in the Curie points and a noticeable decrease in the dc conductivity.<sup>18</sup> At B sites, substitution between niobium and tantalum ions was widely studied.<sup>19–21</sup> Takenaka *et al.* reported the effects of partial substitution of  $\text{Nb}^{5+}$  for  $\text{Ti}^{4+}$  as B-site ions on the formation of layer structure for  $m \geq 3$  compounds and found a BLSFs series for  $m=3$ .<sup>22</sup> Among the BLSFs, SBT and SBN have been the best candidates for nonvolatile memory device because of their fatigue-free properties.<sup>23–26</sup> Another widely studied BLSF material, bismuth titanate,  $\text{Bi}_4\text{Ti}_3\text{O}_{12}$  (BIT) presents very high remanent polarization and thus is also very attractive for memory applications.<sup>27,28</sup> However, BIT

also suffers from the fatigue problem. Park *et al.* reported that the fatigue-free properties of BIT after  $10^{10}$  cycles were achieved by substituting certain bismuth ions with lanthanum.<sup>29</sup> The similar influence of substituting or doping effect in BLSFs was also widely reported in the improvement of ferroelectric properties in isotropic perovskite ferroelectrics.<sup>30</sup>

Recently, we reported that vanadium doping had a significant influence on the dielectric and ferroelectric properties of SBT and SBN systems.<sup>31–36</sup> Particularly, the remanent polarizations of SBN ferroelectric doped with 10 at % vanadium increased from  $\sim 2.8$  to  $\sim 8 \mu\text{C}/\text{cm}^2$  and the coercive field reduced from  $\sim 63$  to  $\sim 50 \text{ kV}/\text{cm}$ . Such an improvement in ferroelectric properties was ascribed to the increased “rattling space.” Vanadium doping also resulted in a noticeable change in dielectric and electrical properties. Further studies on the A-site substitution by ions with various sizes and amounts in the SBN ferroelectric were also carried. It was found that dielectric and electrical properties changed with the type and amount of doping ions. In this article, we present a systematic study on the doping effects on the lattice constants, microstructure, dielectric, and electrical properties of SBN ferroelectric ceramics. Specifically, we studied the partial substitution of  $\text{Nb}^{5+}$  (B site) by  $\text{V}^{5+}$ , and  $\text{Sr}^{2+}$  (A site) by  $\text{Ca}^{2+}$  and  $\text{Ba}^{2+}$ . The relationships between the size of doping ions, dielectric, and electrical properties of SBN ferroelectric ceramics were discussed.

### II. EXPERIMENT

Polycrystalline strontium bismuth vanadium niobate ceramic samples with a composition of  $\text{SrBi}_2(\text{V}_x\text{Nb}_{1-x})_2\text{O}_9$  (SBVN) with  $x$  ranging from 0 to 0.3 and  $(\text{Ca}_x\text{Sr}_{1-x})\text{Bi}_2\text{Nb}_2\text{O}_9$  [(CSBN),  $0 \leq x \leq 0.3$ ] and  $(\text{Ba}_x\text{Sr}_{1-x})\text{Bi}_2\text{Nb}_2\text{O}_9$  [(BSBN),  $0 \leq x \leq 0.3$ ] were prepared by solid-state reaction sintering. The starting materials used were  $\text{SrCO}_3$ ,  $\text{CaCO}_3$ ,  $\text{BaCO}_3$ ,  $\text{Bi}_2\text{O}_3$ ,  $\text{V}_2\text{O}_5$ , and  $\text{Nb}_2\text{O}_5$  (Aldrich Chem. Co.), all with a purity of 99%. The powders were admixed with a desired weight ratio with approximately 4.5 wt % excess  $\text{Bi}_2\text{O}_3$ , which was to compensate the weight loss of  $\text{Bi}_2\text{O}_3$ , due to its high vapor pressure. The

<sup>a)</sup>Electronic mail: gzc@u.washington.edu

vapor pressure of bismuth oxide (750 mm Hg at 1570 °C) is on the order of that of lead oxide (750 mm Hg at 1760 °C).<sup>37</sup> Powders were ball milled with acetone for 24 h and the mixtures were dried at 150 °C for 6 h. The mixtures were then fired in air for 2 h at 850 °C for samples containing 5–10 at% vanadium and 900 °C for base SBN and Ca/Ba doped SBN samples, respectively. The fired powders formed a single phase of the layered perovskite structure with negligible weight loss. The powders were ground and admixed with about 1–1.5 wt% polyvinylalcohol (Aldrich Chem. Co.) as a binder and pressed into pellets uniaxially at ~300 MPa. The pellets were sintered in closed crucibles at 950 °C for 2 h for samples with vanadium dopings and at 1150 °C for 2 h for base SBN and Ca/Ba doped SBN samples in air. All sintered pellets had a relative density above 94% and a single phase layered perovskite structure. After the weight loss from the decompositions of carbonates was excluded, the total weight loss in all samples was found to be less than 3 wt%, which was presumably due to the evaporation of Bi<sub>2</sub>O<sub>3</sub>, but was less than the excess Bi<sub>2</sub>O<sub>3</sub> initially added. The effect of the extra 1.5 wt% Bi<sub>2</sub>O<sub>3</sub> on the physical properties would be the same in all the samples and, thus, is neglected hereinafter in discussing the influences of doping. Further, it was found that the addition of vanadium oxide lowered the sintering temperature approximately 200 °C, while an appreciably higher density was achieved. The lowered sintering temperature in this study is partly due to the low melting point of vanadium oxide (~690 °C), which was also reported as one effective sintering aid for low-firing ceramics,<sup>38,39</sup> and partly due to the possible formation of an eutectic liquid phase in this multiple oxide system. Prior to characterization and property measurements, all the samples with vanadium doping were annealed in oxygen at 800 °C for 3 h.

X-ray diffraction [(XRD) Philips 1830] was used to determine the formation of the desired layered perovskite phase, for both the powders and the pellets. The XRD spectrum of a NaCl crystal was used as a standard to calibrate the scanning angles. The step size of the scan was 0.04/°2θ with a scanning speed of 0.004 °2θ/s. The pseudotetragonal (200) and (1110) peaks were chosen for the lattice constant calculation, which is commonly used in the calculation of a SrBi<sub>2</sub>(Ta,Nb)<sub>2</sub>O<sub>9</sub> (SBTN) system.<sup>40</sup> The microstructure of the sintered samples was analyzed by scanning electron microscopy [(SEM), JEOL 5200] and optical microscopy. Both polished surface and fracture cross section were analyzed, though only the SEM images of fracture surfaces are shown. All of the ceramic pellets were polished to have flat and parallel surfaces and about 1 mm in thickness, electroded by silver paste on both sides, and cured at 550 °C for half an hour. The dielectric properties and ac impedance properties were characterized by a HP 4284A Precision LCR meter (Hewlett Packard Co.). The grain (bulk) conductivities were derived from the impedance results.

### III. RESULTS AND DISCUSSION

#### A. Lattice constants and microstructures

XRD analyses indicated that single phase layered perovskites were formed within the composition ranges studied

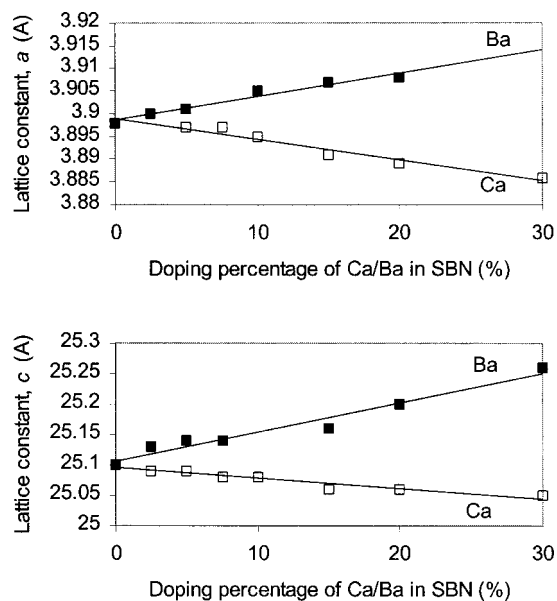


FIG. 1. Lattice constants vs Ca/Ba doping content.

in this work and no secondary phase was detectable. Figure 1 shows the lattice constants as functions of doping content of BaO and CaO. Figure 2 is the lattice constants of SBVN samples as a function of vanadium content. Doping of Ba and Ca resulted in a linear increase or decrease in lattice constants, depending on the dopant ionic radii relative to that of Sr<sup>2+</sup>. However, V<sub>2</sub>O<sub>5</sub> doping demonstrated a different influence on the lattice constants. The change of lattice constants are significantly smaller than that in the CSBN and BSBN systems. Further, there is almost no change in the *c* axis, whereas the *a* axis remains the same until the doping content exceeds 15 at%. This might suggest that the constraint introduced by the [Bi<sub>2</sub>O<sub>2</sub>]<sup>2+</sup> interlayer exerts different degrees of influences on the structure change upon doping at A and B sites. At room temperature, SBN, CaBi<sub>2</sub>Nb<sub>2</sub>O<sub>9</sub> (CBN), and BaBi<sub>2</sub>Nb<sub>2</sub>O<sub>9</sub> (BBN) have an orthorhombic struc-

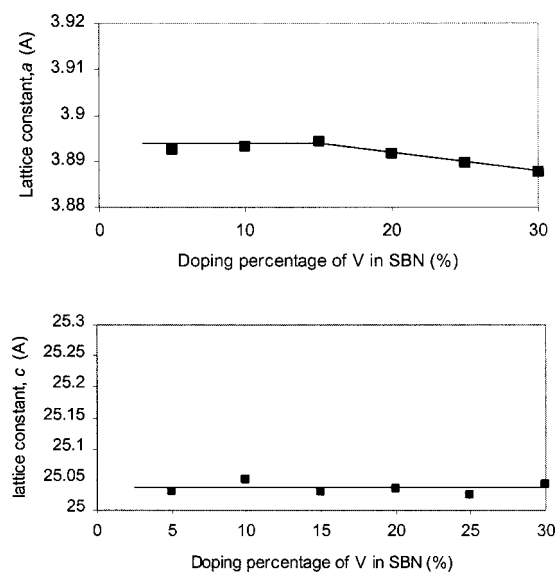


FIG. 2. Lattice constants vs vanadium doping content.

TABLE I. Deduced and reported Curie temperatures and lattice constants of CBN and BBN.

Sample	$T_C$ (literature, °C)	$T_C$ (extrapolated, °C)	Extrapolated $a, c$ (Å)	Reported $a, c$ (Å)
SBN	~420	...	...	$a \sim 3.901$ ; $c \sim 25.1124$
CBN	~620	~910	$a \sim 3.8589$ ; $c \sim 24.925$	$a \sim 3.8540$ ; $c \sim 24.97$
BBN	~200	~90	$a \sim 3.9486$ ; $c \sim 25.586$	$a \sim 3.9365$ ; $c \sim 25.634$

ture which is maintained with various doping of  $\text{Ba}^{2+}$  and  $\text{Ca}^{2+}$  for  $\text{Sr}^{2+}$  and  $\text{V}^{5+}$  for  $\text{Nb}^{5+}$  in the SBN system. It is noticed that for all three compounds, their lattice constants  $a$  and  $b$  are very close. Therefore, in our discussion, a pseudotetragonal cell was used for the sake of simplicity and clarity by assuming  $a = (a_0 + b_0)/2\sqrt{2}$  (Ref. 26) and using the same  $c$  value. So,  $a = 3.901 \text{ \AA}$  for SBN (our XRD result is  $\sim 3.898 \text{ \AA}$ ),  $3.8540 \text{ \AA}$  for CBN, and  $3.9365 \text{ \AA}$  for BBN. From Fig. 1, by extrapolating the linear relationship observed with relatively low doping, the lattice constants for CBN could be deduced:  $a = 3.8589 \text{ \AA}$  and  $c = 24.925 \text{ \AA}$ , and for BBN:  $a = 3.948 \text{ \AA}$  and  $c = 25.586 \text{ \AA}$ . Table I summarized the lattice constants reported in the literature<sup>41–43</sup> and those extrapolated from Fig. 1. It is found that the lattice constants extrapolated are close to the data reported in literature. The small deviation could be attributed at least partly to the possible measurement errors. It was further found that the change in barium doped samples is more appreciable than calcium and vanadium. One possible explanation is that barium is much bigger than strontium, whereas the size difference between  $\text{Ca}^{2+}$  and  $\text{Sr}^{2+}$  ions is relatively small. The ionic radii and tolerance factors of SBN, BBN, CBN, and hypothetical strontium bismuth vanadate,  $\text{SrBi}_2\text{V}_2\text{O}_9$  (SBV) samples are summarized in Table II. It is also interesting to compare the tolerance factors of BBN and SBV. Although SBV has a tolerance factor of 1.02, close to 1, and smaller as compared to BBN (1.04), no stable SBV compound was synthesized,<sup>32</sup> whereas BBN forms a stable layer-structured perovskite. No explanation is available; however, it is most likely due to the structural constraint imposed by the  $[\text{Bi}_2\text{O}_2]^{2+}$  interlayers.

Figure 3 shows the SEM images of fracture surfaces of SBN ceramics without doping and doped with 5 at % CaO, BaO, and  $\text{V}_2\text{O}_5$ , respectively. There are no apparent differences in microstructures between SBN and calcium or barium doped samples. However, with vanadium doping, the grain sizes ( $\sim 1 \mu\text{m}$ ) were about 2–3 times smaller as com-

pared to undoped SBN ceramics (2–3  $\mu\text{m}$ ). This could be attributed to the lower sintering temperature ( $\sim 200^\circ\text{C}$  lower) of vanadium doped samples and similar results were obtained in vanadium doped SBT samples.<sup>36</sup> Further, it was found that there was no appreciable influence of doping content on microstructures.

## B. Curie temperatures

Figure 4(a) shows the Curie temperatures of SBN doped with various amounts of CaO and BaO, and good linear relationships were observed. The Curie temperature increases with an increasing Ca doping level, whereas the Curie temperature decreases with an increasing Ba doping level. This linear relationship further suggests that the crystal structure of the SBN layer perovskite remains unchanged with  $\text{Ca}^{2+}$  and  $\text{Ba}^{2+}$  doping. The influence on Curie temperature by vanadium doping in SBN is shown in Fig. 4(b). The Curie temperature is also found to increase almost linearly with an increasing vanadium content.

Generally, ferroelectrics with a large ionic displacement would have a high Curie temperature, a large spontaneous polarization, and a large coercive field. The ionic displacement could be influenced by several factors including the ionic size, tolerance factor, ionic polarizability, etc.<sup>44</sup> In isotropic perovskite ferroelectrics, doping with bigger A-site ions and/or smaller B-site ions usually leads to a higher Curie temperature. For example, the Curie temperature of  $(\text{Ba}, \text{Sr})\text{TiO}_3$  changes linearly with the Ba/Sr ratio, and a lower Zr/Ti ratio leads to a higher Curie temperature of  $\text{Pb}(\text{Zr}, \text{Ti})\text{O}_3$  systems. This could be understood by larger rattling space for the B-site ions in the center of perovskite units. Further,  $\text{Pb}^{2+}$  and  $\text{Bi}^{3+}$  usually lead to relatively high Curie temperatures, possibly because they have a pair of 6s-electrons beyond the closed shell.<sup>7</sup> This lone pair of electrons might contribute to the polarizations. So,  $\text{Pb}^{2+}$  and  $\text{Ti}^{4+}$  in  $\text{PbTiO}_3$  possess higher ionic displacement data compared with that of  $\text{Ba}^{2+}$  and  $\text{Ti}^{4+}$  in  $\text{BaTiO}_3$  (Ref. 30) and much higher Curie temperature than  $\text{BaTiO}_3$  even though  $\text{Ba}^{2+}$  ( $\sim 160 \text{ pm}$ ) is bigger than  $\text{Pb}^{2+}$  ( $\sim 132 \text{ pm}$ ).

In layer-structured perovskites, the crystal structure may not change as freely as that of isotropic perovskites with doping due to the structural constraint imposed by the  $[\text{Bi}_2\text{O}_2]^{2+}$  interlayer. When  $\text{Sr}^{2+}$  ( $\sim 143 \text{ pm}$ ) in the A site is substituted by a larger ion ( $\text{Ba}^{2+}$ ) ( $\sim 160 \text{ pm}$ ), the Curie temperature decreases. When a smaller ion,  $\text{Ca}^{2+}$  ( $\sim 136 \text{ pm}$ ) substitutes  $\text{Sr}^{2+}$ , the Curie temperature increases. This might suggest that with the bismuth layer structural constraint, the introduction of bigger ions into A sites would eventually consume more space despite the lattice increase. As a result, the rattling space for the ions inside the oxygen octahedral

TABLE II. Summary of ionic radii, coordination numbers, and tolerance factor of layer perovskite  $\text{ABi}_2\text{B}_2\text{O}_9$ ,  $r_o^{2+} = 1.40 \text{ \AA}$  [coordination number (CN) = 6].<sup>a</sup>

Ion site	Ions	Radius (Å)	CN	Tolerance factor
A (B=Nb)	$\text{Sr}^{2+}$	1.44	12	0.98
	$\text{Ca}^{2+}$	1.36	12	0.95
	$\text{Ba}^{2+}$	1.60	12	1.04
B (A=Sr)	$\text{Nb}^{5+}$	0.69	6	0.98
	$\text{V}^{5+}$	0.58	6	1.02

<sup>a</sup>See Ref. 46.



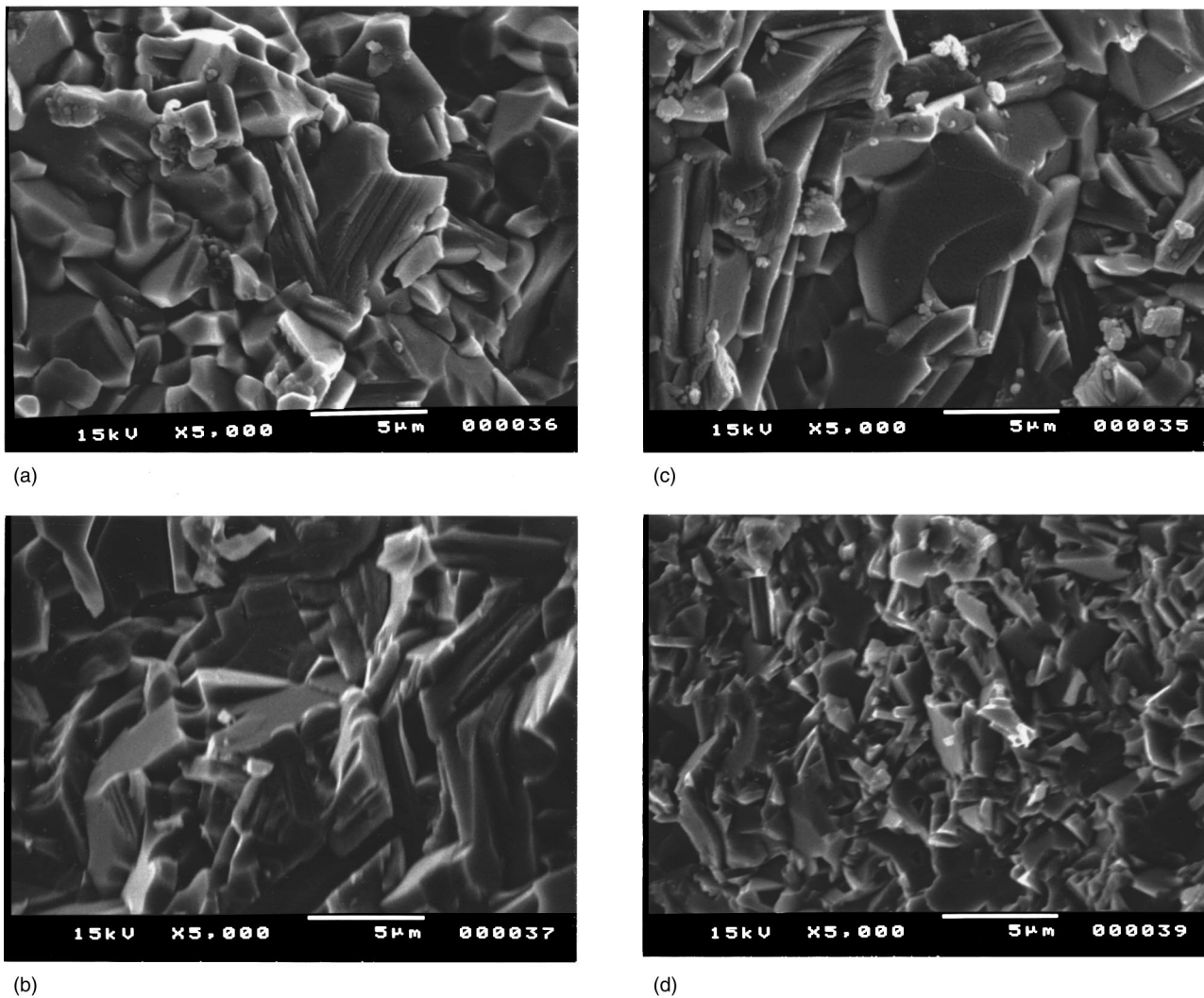


FIG. 3. SEM pictures of SBN and Ca/Ba/V doped ceramics: (a) without doping, (b) doped with 5 at.% Ca, (c) doped with 5 at.% Ba, and (d) doped with 5 at.% V.

would be reduced and the Curie temperature would decrease. Assuming the linear relationship between  $T_C$  and doping content holds, the extrapolated  $T_C$  for CBN and BBN compounds would be approximately 910 °C and 90 °C, respectively. However, the  $T_C$  for CBN and BBN compounds are reported to be ~620 °C<sup>44</sup> and 200 °C,<sup>26</sup> respectively. The extrapolated and/or reported Curie temperatures of SBN, BBN, and CBN are also summarized in Table I. In contrast to the linear relationship between the lattice constants and chemical composition, the significant difference between extrapolated  $T_C$  and literature reported data strongly suggests that linear relationship observed at a low doping level does not persist throughout the whole composition range. This result probably could be understood by considering the fact that Curie temperature is related to ionic polarizability, which is closely related to structural displacement distortion. The bigger differences in the  $a$ ,  $b$  values of CBN as compared to that of SBN and BBN corroborate its higher Curie point.<sup>41-43</sup>

Figure 4(b) shows the Curie temperature ( $T_C$ ) as a function of vanadium content. The Curie point gradually increases with an increasing vanadium concentration, which could be again an indication that a single phase layered per-

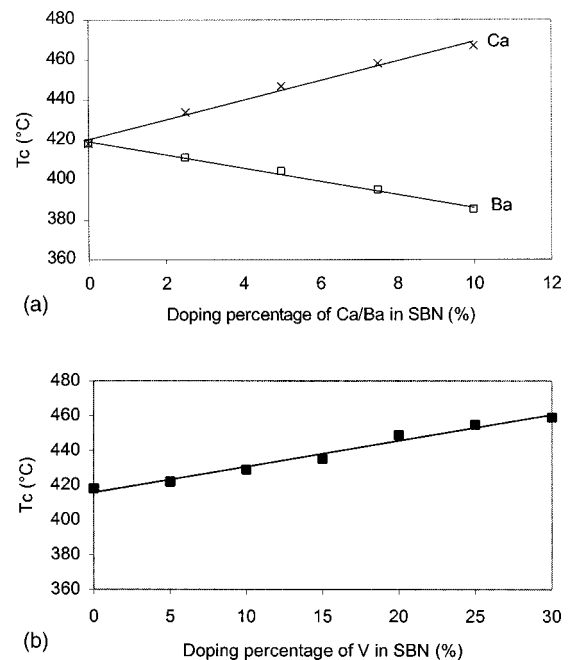


FIG. 4. Curie temperature vs Ca/Ba doping content (a) and Curie temperature vs vanadium doping content (b).

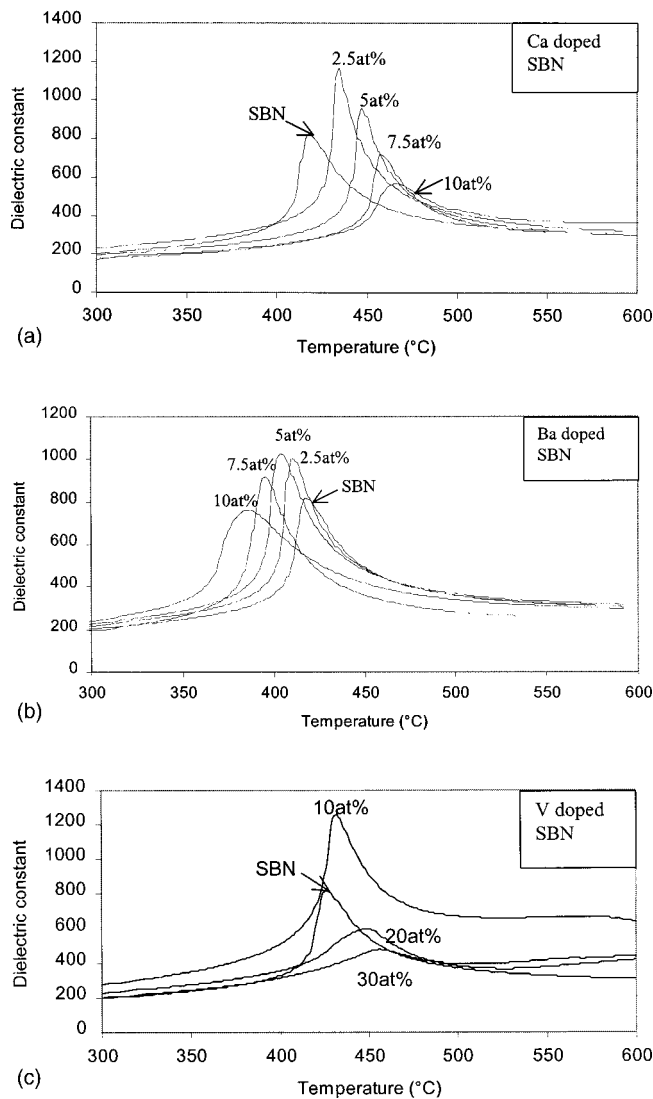


FIG. 5. Dielectric constants at 100 kHz vs temperature in Ca doped (a), Ba doped (b), and V doped SBN systems (c).

ovskite was formed with up to 30 at % vanadium substitution. In general, the increase in Curie temperature in the system below 15 at % is thought to be mainly due to the smaller vanadium ions substitution for niobium with almost unchanged unit cell volume (Fig. 2). Above 15 at %, the increase in the Curie temperature corresponds to a reduced unit cell volume. It is noticed that the increase in the Curie temperature shows a slight discontinuity between 15 and 20 at % of vanadium doping, however, no explanation is available at the moment to our knowledge.

### C. Dielectric properties

Figure 5 shows the dielectric constants of SBN ceramics doped with various types and amounts of dopants as a function of temperature, determined at a frequency of 100 kHz with an oscillation amplitude of 50 mV. All plots show a peak maximal dielectric constant at certain composition (CSBN ~ 2.5 at %, BSBN ~ 5 at %, and SBVN ~ 10 at %).

Under the measurement conditions (100 kHz and 50 mV) used in this study, the dielectric constants of SBN re-

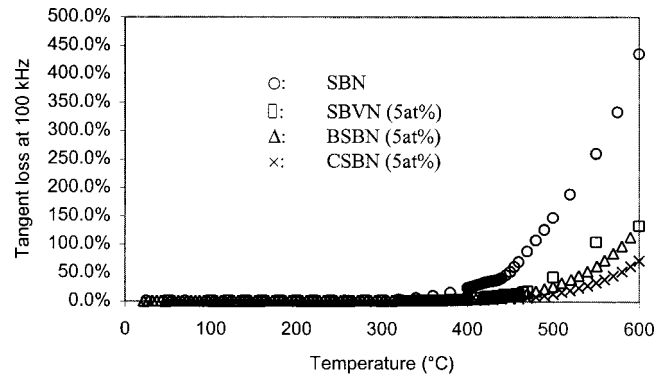


FIG. 6. Tangent loss at 100 kHz vs temperature in SBN (O) and 5 at % Ca (x), 5 at % Ba ( $\Delta$ ), and 5 at % V ( $\square$ ) doped SBN systems.

gardless of doping only consist of ionic and atomic polarization. Since the ionic radii of doping ions ( $\text{Ca}^{2+}$ ,  $\text{Ba}^{2+}$ , and  $\text{V}^{5+}$ ) are different from the original site ions ( $\text{Sr}^{2+}$  and  $\text{Nb}^{5+}$ ),<sup>45</sup> increasing the amount of doping ions would lead to a change of both electronic and ionic polarization. Ionic polarization is strongly dependent on the crystal structure, including density and lattice constant or unit cell volume. Considering vanadium doping, when the concentration of  $\text{V}^{5+}$  is less than 15 at %, the lattice constants or unit cell volumes remain almost unchanged as demonstrated in Fig. 2. As a result, there would be an increased ionic polarization with an increased  $\text{V}^{5+}$  concentration, due to a combination of unchanged unit cell volume and reduced ionic radius. An increase in dielectric constant indicates that the increase in ionic polarization is predominant over the decrease in electronic polarization corresponding to smaller ionic radius. However, a high concentration of vanadium caused a reduction in the lattice constants and unit cell volume (as shown in Fig. 2). Therefore, both atomic and ionic polarization would decrease with an increasing amount of vanadium introduced into the system and lead to reduced dielectric constants.

The tangent losses as a function of temperature at 100 kHz for SBN with and without doping are shown in Fig. 6. Tangent losses increase with increasing temperatures particularly at temperatures higher than  $\sim 400^\circ\text{C}$ . This could be caused by a higher concentration of charge carriers (positive and negative vacancies) at higher temperatures. It is also noticed that with partial doping (5 at %), the tangent losses decrease, especially at high temperatures. This might be related to the increased complexity in the crystal structure via doping and will be discussed more in the following section.

### D. Electrical conductivities

Figure 7 shows the bulk conductivities of SBN and doped samples determined by the ac impedance analyses. The temperature range ( $\sim 300^\circ\text{C}$ – $\sim 700^\circ\text{C}$ ) likely corresponds to the intrinsic ionic conduction range and the conduction is presumably dominated by the intrinsic defects. The incorporation of dopants resulted in reduced dc conductivities, regardless of the types and amounts of dopants.

For a single phase material with a homogenous microstructure, the electrical conductivity,  $\sigma$ , depends on both the

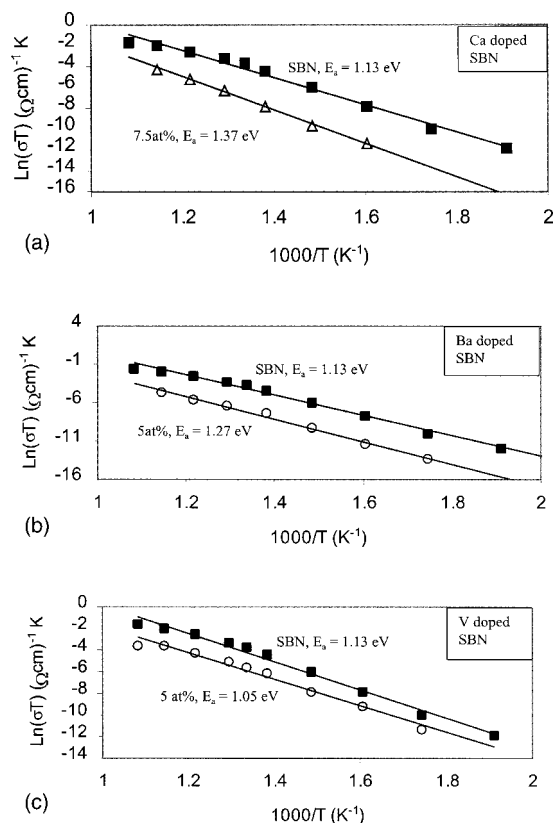


FIG. 7. Bulk conductivities of Ca doped (a), Ba doped (b), and V doped SBN systems (c).

concentration and mobility of charge carriers and can be presented by the following simplified equation:<sup>46</sup>

$$\sigma = nq\mu = (A/T)\exp(-E_a/kT), \quad (1)$$

where  $n$  is the concentration of charge carriers,  $q$ , the number of charges per charge carrier,  $\mu$ , the mobility of charge carriers,  $A$ , a temperature-independent constant,  $E_a$ , the nominal activation energy per charge carrier,  $k$ , the Boltzmann's constant, and,  $T$ , the temperature. At low temperatures, when the extrinsic conduction is predominant, the nominal activation energy is equal to the diffusion activation energy. However, at high temperatures when intrinsic conduction predominates, the nominal activation is the sum of diffusion activation,  $E_d$ , and the formation energy of charge carrier,  $E_f$ :

$$E_a = E_d + E_f. \quad (2)$$

According to Eq. (1), a reduced dc conductivity suggests a reduced concentration and/or mobility of charge carriers.

It is found that the dc conductivity at a high temperature ( $\sim 300^\circ\text{C}$ – $\sim 700^\circ\text{C}$ ) of the SBN ceramics decreased with A or B site doping, and there was also an appreciable change in activation energy for SBN and doped samples. Table III summarizes the activation energies and dc conductivities of SBN and doped samples at  $500^\circ\text{C}$ . Based on the activation energy data, the conduction is likely due to the migration of oxygen vacancies.<sup>47–49</sup> A decrease in activation energy with an increasing amount of vanadium doping, however, suggests that the concentration of intrinsic charge carriers may increase

TABLE III. dc conductivity and activation energies of SBN and doped samples.

Sample	$E_a$ (eV)	$\sigma_{dc}$ at $500^\circ\text{C}$ (S/cm)
SBN ( $X=0$ )	1.13	$\sim 4.84 \times 10^{-5}$
SBVN ( $X=0.05$ )	1.05	$\sim 8.56 \times 10^{-6}$
CSBN ( $X=0.075$ )	1.37	$\sim 2.42 \times 10^{-6}$
BSBN ( $X=0.05$ )	1.27	$\sim 2.09 \times 10^{-6}$

due to the incorporation of vanadium cations. If the primary intrinsic charge carriers in the layered perovskite ferroelectrics are oxygen vacancies, a relatively lower diatomic bond strength of V—O bonds ( $\sim 627$  kJ/mol), as compared to that of Nb—O bonds ( $\sim 703$  kJ/mol),<sup>36</sup> could be responsible for the reduced activation energy with vanadium doping. Barium doping introduces a higher activation energy. Stronger Ba—O bonds ( $\sim 562$  kJ/mol) compared to Sr—O bonds ( $\sim 426$  kJ/mol) might be the reason. However, with weaker Ca—O bonds ( $\sim 402$  kJ/mol) compared to Sr—O bonds, it is hard to explain why calcium doped samples also show higher activation energies. The experimental results observed in this study suggest that the effects of A site (Ca/Ba) and B site (V) dopings on the dc conduction are complex, and further analysis is required to achieve a better understanding.

#### IV. SUMMARY

Doping in layer-structured SBN ceramics was found to have significant influences on dielectric and electric properties. Depending on the ionic radii of dopants, the lattice constant and Curie temperature either increase or decrease with and increasing amount of dopants, which is similar to what was reported in isotropic perovskite ferroelectrics in literature. Dielectric constants initially increase with a small amount of dopant, regardless of the types of dopants, and reach a maximum at a doping level between 2.5–15 at %. It was also found that doping resulted in a reduced tangent loss and bulk conductivity at temperatures ranging from room temperature to  $\sim 600^\circ\text{C}$ , regardless of the types of dopants at the doping level ( $<10$  at %) studied in this research.

#### ACKNOWLEDGMENTS

Two of the authors (Y.W. and S.S.) would like to acknowledge the Center for nanotechnology at University of Washington for financial support. S.J.L. would like to thank NSF-IGERT and Pacific Northwest National Laboratories for partial financial support.

<sup>1</sup>B. Aurivillius, *Ark. Kemi* **1**, 449 (1951); **2**, 519 (1951).  
<sup>2</sup>J. F. Scott and C. A. P. de Araujo, *Science* **246**, 1400 (1989).  
<sup>3</sup>G. Z. Cao, in *Advances in Materials Science and Applications*, edited by D. L. Shi (TUP and Springer, Beijing, 2001), p. 86.  
<sup>4</sup>R. E. Jones, Jr., P. D. Maniar, R. Moazzami, P. Zurcher, J. Z. Witowski, Y. T. Lii, P. Chu, and S. J. Gillespie, *Thin Solid Films* **270**, 584 (1995).  
<sup>5</sup>J. Robertson, C. W. Chen, W. L. Warren, and C. C. Gutleben, *Appl. Phys. Lett.* **69**, 1704 (1996).  
<sup>6</sup>P. Millan, A. Ramirez, and A. Castro, *J. Mater. Sci. Lett.* **14**, 1657 (1995).  
<sup>7</sup>P. Duran-Martin, A. Castro, P. Millan, and B. Jimenez, *J. Mater. Res.* **13**, 2565 (1998).  
<sup>8</sup>P. Millan, A. Castro, and J. B. Torrance, *Mater. Res. Bull.* **28**, 117 (1993).

- <sup>9</sup>T. Atsuki, N. Soyama, T. Yonezawa, and K. Ogi, *Jpn. J. Appl. Phys.*, Part 1 **34**, 5096 (1995).
- <sup>10</sup>T. Noguchi, T. Hase, and Y. Miyasaka, *Jpn. J. Appl. Phys.*, Part 1 **35**, 4900 (1996).
- <sup>11</sup>H. Tsai, P. Lin, and T. Tseng, *Appl. Phys. Lett.* **72**, 1787 (1998).
- <sup>12</sup>E. C. Subbarao, *Phys. Rev.* **122**, 804 (1961).
- <sup>13</sup>E. C. Subbarao, *J. Chem. Phys.* **34**, 695 (1961).
- <sup>14</sup>E. C. Subbarao, *J. Phys. Chem. Solids* **23**, 665 (1962).
- <sup>15</sup>R. E. Newnham, R. W. Wolfe, R. S. Horsey, F. A. Diaz-Colon, and M. I. Kay, *Mater. Res. Bull.* **8**, 1183 (1973).
- <sup>16</sup>C. H. Lu and C. Y. Wen, *Mater. Res. Soc. Symp. Proc.* **541**, 229 (1999).
- <sup>17</sup>C. H. Lu and C. Y. Wen, *J. Eur. Ceram. Soc.* **20**, 739 (2000).
- <sup>18</sup>M. J. Forbess, S. Seraji, Y. Wu, C. P. Nguyen, and G. Z. Cao, *Appl. Phys. Lett.* **76**, 2934 (2000).
- <sup>19</sup>H. Watanabe, T. Mihara, H. Yoshimori, and C. A. de Araujo, *Jpn. J. Appl. Phys.*, Part 1 **34**, 5240 (1995).
- <sup>20</sup>S. B. Desu and D. P. Vijay, *Mater. Sci. Eng.*, B **32**, 83 (1995).
- <sup>21</sup>S. B. Desu and T. Li, *Mater. Sci. Eng.*, B **34**, L4 (1995).
- <sup>22</sup>T. Takenaka, T. Gotoh, S. Mutoh, and T. Sasaki, *Jpn. J. Appl. Phys.*, Part 1 **34**, 5384 (1995).
- <sup>23</sup>C. A. P. de Araujo, J. D. McMillan, M. C. Scott, and J. F. Scott, *Nature (London)* **374**, 627 (1995).
- <sup>24</sup>T. Mihara, H. Yoshimori, H. Watanabe, and C. A. P. de Araujo, *Jpn. J. Appl. Phys.*, Part 1 **34**, 5233 (1995).
- <sup>25</sup>J. F. Scott, in *Thin Film Ferroelectric Materials and Devices*, edited by R. Ramesh (Kluwer, Norwell, MA, 1997), p. 115.
- <sup>26</sup>M. Suzuki, *J. Ceram. Soc. Jpn.* **103**, 1088 (1995).
- <sup>27</sup>R. E. Newnham, R. W. Wolfe, and J. F. Dorrian, *Mater. Res. Bull.* **6**, 1029 (1971).
- <sup>28</sup>J. F. Dorrian, R. E. Newnham, D. K. Smith, and M. I. Kay, *Ferroelectrics* **3**, 17 (1971).
- <sup>29</sup>B. H. Park, B. S. Kang, S. D. Bu, T. W. Noh, J. Lee, and W. Jo, *Nature (London)* **401**, 682 (1999).
- <sup>30</sup>Y. H. Xu, *Ferroelectric Materials and Their Applications* (Elsevier Science, Amsterdam, 1991).
- <sup>31</sup>Y. Wu, C. Nguyen, S. Seraji, M. J. Forbess, S. J. Limmer, T. P. Chou, and G. Z. Cao, *J. Am. Ceram. Soc.* (to be published).
- <sup>32</sup>Y. Wu and G. Z. Cao, *J. Mater. Res.* **15**, 1583 (2000).
- <sup>33</sup>Y. Wu and G. Z. Cao, *Appl. Phys. Lett.* **75**, 2650 (1999).
- <sup>34</sup>Y. Wu and G. Z. Cao, *J. Mater. Sci. Lett.* **19**, 267 (2000).
- <sup>35</sup>Y. Wu, M. Forbess, S. Seraji, S. Limmer, T. Chou, and G. Z. Cao, *J. Appl. Phys.* **89**, 5647 (2001).
- <sup>36</sup>Y. Wu, M. Forbess, S. Seraji, S. Limmer, T. Chou, and G. Z. Cao, *Mater. Sci. Eng.*, B **86**, 70 (2001).
- <sup>37</sup>*CRC Handbook of Chemistry and Physics*, 61st ed., edited by R. C. Weast and M. J. Astle (CRC, Boca Raton, FL, 1974).
- <sup>38</sup>C. Kuo, C. Chen, and I. Lin, *J. Am. Ceram. Soc.* **81**, 2942 (1998).
- <sup>39</sup>K. B. R. Varma and K. V. R. Prasad, *J. Mater. Res.* **11**, 2288 (1996).
- <sup>40</sup>Y. Torii, K. Tato, A. Tsuzuki, H. J. Hwang, and S. K. Dey, *J. Mater. Sci. Lett.* **17**, 827 (1998).
- <sup>41</sup>Ismunandar, B. J. Kenedy, Gunawan, and Marsongkohadi, *J. Solid State Chem.* **126**, 135 (1996).
- <sup>42</sup>S. B. Desu, H. S. Cho, and P. C. Joshi, *Appl. Phys. Lett.* **70**, 1393 (1997).
- <sup>43</sup>C. R. Foschini, P. C. Joshi, J. A. Varela, and S. B. Desu, *J. Mater. Res.* **14**, 1860 (1999).
- <sup>44</sup>V. A. Isupov, *Inorg. Mater. (Transl. of Neorg. Mater.)* **33**, 936 (1997).
- <sup>45</sup>R. D. Shannon and C. T. Prewitt, *Acta Crystallogr., Sect. B: Struct. Crystallogr. Cryst. Chem.* **25**, 925 (1969).
- <sup>46</sup>A. J. Moulson and J. M. Herbert, *Electroceramics* (Chapman and Hall, London, 1990).
- <sup>47</sup>A. Chen, Y. Zhi, and L. E. Cross, *Phys. Rev. B* **62**, 228 (2000).
- <sup>48</sup>Y. Zhi, A. Chen, P. M. Vilarinho, P. Mantas, and J. L. Baptista, *J. Appl. Phys.* **83**, 4874 (1998).
- <sup>49</sup>R. Waser, *J. Am. Ceram. Soc.* **74**, 1934 (1991).